TU/e EINDHOVEN UNIVERSITY OF TECHNOLOGY

In situ crystallization kinetics studies of plasma-deposited, hydrogenated amorphous silicon layers

Citation for published version (APA):
Sharma, K., Verheijen, M. A., Sanden, van de, M. C. M., & Creatore, M. (2012). In situ crystallization kinetics studies of plasma-deposited, hydrogenated amorphous silicon layers. *Journal of Applied Physics*, *111*(3), 033508-1/6. [033508]. https://doi.org/10.1063/1.3681185

DOI:
10.1063/1.3681185

Document status and date:
Published: 01/01/2012

Document Version:
Publisher's PDF, also known as Version of Record (includes final page, issue and volume numbers)

Please check the document version of this publication:

• A submitted manuscript is the version of the article upon submission and before peer-review. There can be important differences between the submitted version and the official published version of record. People interested in the research are advised to contact the author for the final version of the publication, or visit the DOI to the publisher's website.
• The final author version and the galley proof are versions of the publication after peer review.
• The final published version features the final layout of the paper including the volume, issue and page numbers.

Link to publication

General rights
Copyright and moral rights for the publications made accessible in the public portal are retained by the authors and/or other copyright owners and it is a condition of accessing publications that users recognise and abide by the legal requirements associated with these rights.

• Users may download and print one copy of any publication from the public portal for the purpose of private study or research.
• You may not further distribute the material or use it for any profit-making activity or commercial gain
• You may freely distribute the URL identifying the publication in the public portal.

If the publication is distributed under the terms of Article 25fa of the Dutch Copyright Act, indicated by the "Taverne" license above, please follow below link for the End User Agreement:

www.tue.nl/taverne

Take down policy
If you believe that this document breaches copyright please contact us at:

openaccess@tue.nl

providing details and we will investigate your claim.

Download date: 25. Aug. 2022

In situ crystallization kinetics studies of plasma-deposited, hydrogenated amorphous silicon layers

K. Sharma,[1,a)] M. A. Verheijen,[1] M. C. M. van de Sanden,[1,2] and M. Creatore[1,a)]
[1]*Department of Applied Physics, Eindhoven University of Technology, P. O. Box 513, Eindhoven 5600 MB, Netherlands*
[2]*FOM Institute for Plasma Physics Rijnhuizen, P. O. Box 1207, Nieuwegein 3430 BE, Netherlands*

(Received 25 September 2011; accepted 6 January 2012; published online 6 February 2012)

The impact of the amorphous silicon properties, i.e., the microstructure parameter R^* and the medium range order (MRO), on the crystallization process is highlighted and discussed. In agreement with literature, the development of large grains extending through the thickness of the poly-Si layer is found to be promoted by an increase in the amorphous silicon microstructure parameter, R^*. Furthermore, while the role of the MRO in controlling the incubation time and, therefore, the onset in crystallization is generally acknowledged, it is also concluded that the presence of nano-sized voids plays an essential role in the crystallization kinetics. © *2012 American Institute of Physics*. [doi:10.1063/1.3681185]

I. INTRODUCTION

Solid-phase crystallization (SPC) of amorphous silicon (a-Si:H) is nowadays widely investigated and reported in literature, due to the recognized potential of poly-Si as an absorber in thin film photovoltaics.[1] Poly-Si as obtained by SPC of a-Si:H[2–4] is characterized by large grains (~2 μm) and good area uniformity. For example, CSG Solar has reported on a conversion efficiency of 10.4% based on the SPC of a-Si:H layers deposited by plasma-enhanced chemical vapor deposition (PECVD).[3,5]

According to the classical model of nucleation and grain growth, the SPC of a-Si:H follows the three classical steps of (1) incubation (the time before the onset of nucleation), (2) nucleation (creation of random nuclei), and (3) grain growth (where the grain development is in competition with nuclei formation).[6] Several studies have been carried out to determine the effect of the structural properties of a-Si:H on the crystallization process and, in particular, on the nucleation phase.[2,6–14] In order to present an overview of the work reported in literature, we report in Fig. 1 a sketch of an amorphous silicon network, where the hydrogen is present in mono-/divacancies and nano-sized voids.[15–18] IR spectroscopy is a widely known and adopted diagnostic to identify the presence of hydrogen in mono-/divacancies (low stretching mode (LSM) in the range of 1980-2010 cm^{-1}) and in nanosized voids (high stretching mode (HSM) in the range of 2070-2100 cm^{-1}).[15–18] Furthermore, it is essential to define also the ordered regions within the a-Si:H network, as they are reported to control the incubation time in a-Si:H upon annealing,[1] as it will be later addressed. In particular, the short-range order (SRO) is restricted to the region of the silicon network up to a distance of 3 Å from the mono-/divacancies, while the medium-range order (MRO) extends up to 25 Å from the mono-/divacancies.[19–21]

It is generally acknowledged[7,9,12,13] that the development of nuclei in an a-Si:H layer is hampered by the degree of structural disorder, often quantified in terms of the microstructure parameter R^*, defined as $A_{HSM}/(A_{LSM}+A_{HSM})$, where A_{LSM} and A_{HSM} are the integrated absorption areas of the LSM and the HSM, respectively. Recently, we also specifically addressed the relationship between R^* and the grain size development in poly-Si obtained upon SPC of a-Si:H films deposited in a remote plasma configuration, i.e., the expanding thermal plasma (ETP).[22] The grain size in poly-Si was found to increase (from 0.4 μm to 1.5 μm) with increasing R^* (from 0.1 to 0.45).[22] Furthermore, when referring to the crystallization kinetics studies, Mahan *et al.*[1] investigated the development of poly-Si from a-Si:H films deposited by RF capacitively coupled PECVD and hot wire CVD. They identified the nucleation centers to be the hydrogen-deficient regions, i.e., the regions surrounding the hydrogen sites corresponding to a dominant 2000 cm^{-1} peak in the IR spectra. They also reported on the incubation time being controlled by the MRO of the better ordered areas surrounding the same hydrogen sites.

In the present contribution, we proceed further with the investigation of a-Si:H films deposited by means of the ETP-CVD and provide a detailed *in situ* XRD study on the crystallization kinetics during the SPC treatment. Although our results appear to confirm the role of the MRO in controlling the incubation time (t_o), the investigation of an extended R^* range covered by our experimental conditions suggest that the MRO of the pristine a-Si:H layer is not the only parameter accounting for the control of nuclei formation. We show evidence that the pristine a-Si:H microstructure changed upon SPC treatment and that these structural modifications induced a change in the MRO, which eventually affect the incubation time toward poly-Si formation.

II. EXPERIMENTAL

a-Si:H films were deposited on *c*-Si and Si_3N_4-coated glass substrates (Si_3N_4 was used as a diffusion barrier against

a)Authors to whom correspondence should be addressed. Electronic addresses: k.sharma@tue.nl and m.creatore@tue.nl.

 © 2012 American Institute of Physics

Downloaded 23 Apr 2012 to 131.155.151.8. Redistribution subject to AIP license or copyright; see http://jap.aip.org/about/rights_and_permissions

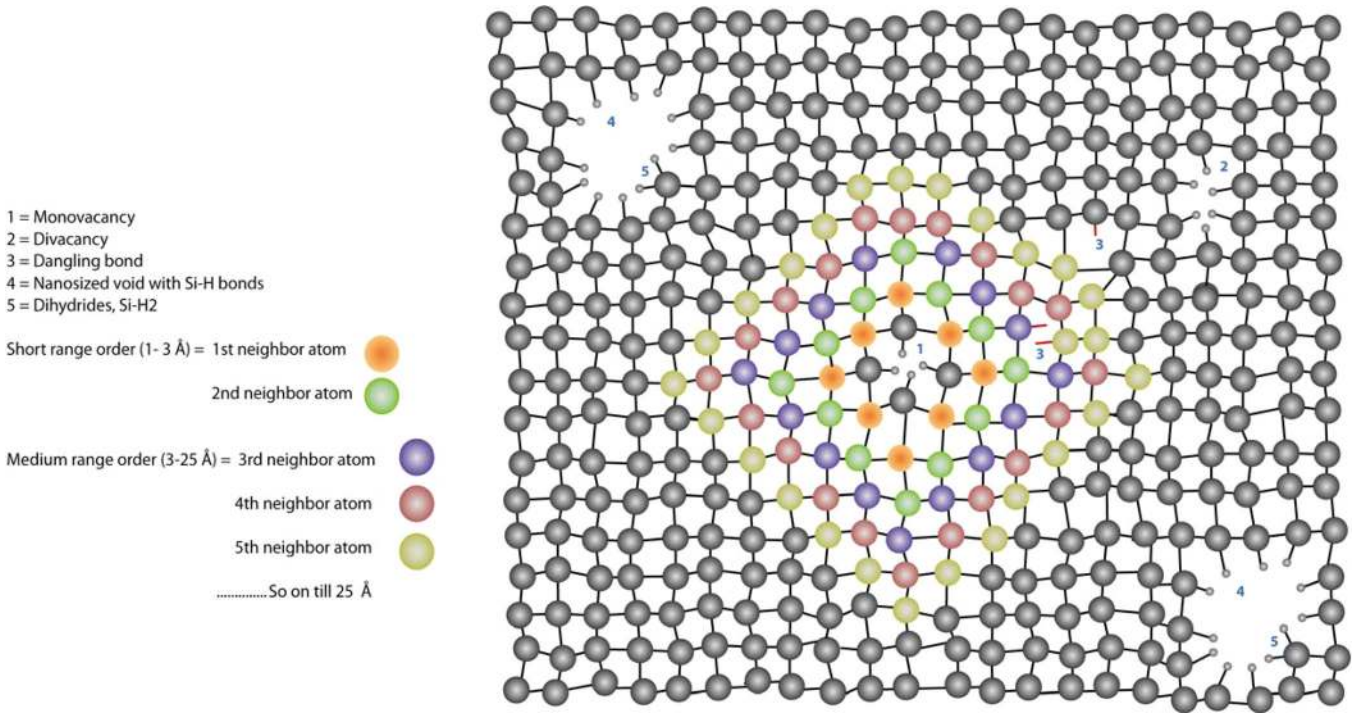

FIG. 1. (Color online) Schematic of an a-Si:H network, where hydrogen in mono-/divacancies and H in nano-sized voids can be identified together with the area covered by the short-range and medium-range order.

impurities from glass) by an expanding thermal plasma (ETP) technique, previously described in detail,[23,24] at substrate temperatures of 200–500 °C. a-Si:H films with a varying R^* at a constant hydrogen content were deposited at each substrate temperature (Table I). The characterization techniques used in this study were Fourier transform infra-red (FTIR) spectroscopy, spectroscopic ellipsometry, Raman spectroscopy, cross-section transmission electron microscopy (XTEM), and x ray diffraction (XRD). *Ex situ* UV-VIS (visable) spectroscopic ellipsometry (SE) (Woollam M-2000U rotating compensator ellipsometer) provided the parameters Ψ and Δ at an angle of incidence of 75° over the spectral range of 245-1000 nm, with a resolution of 1.6 nm. The Cody-Lorentz model[25] was used to determine the thickness and refractive index of the a-Si:H layers. The model (Complete-EASE software, Woollam) consisted of 1) Si substrate, 2) SiO_2 native oxide layer (≈2 nm), and 3) a general oscillator, including a Cody-Lorentz oscillator. The Raman spectra of the samples were recorded using a micro-Raman scattering setup (In-via Renishaw) with a resolution of 1.6 cm^{-1}. The FTIR measurements were carried out using a Bruker Tensor 27 Fourier transform infrared spectrometer. The total hydrogen content (C_H) was calculated from the Si–H wagging mode using a proportionality constant previously reported in literature.[15,26] A Philips X'Pert Pro system was used for the XRD measurements with Cu-Kα x rays selected with a graphite crystal monochromator. The information related to the MRO scale (3–6 Å to as high as 15–25 Å[20,27–30]) were obtained by XRD linewidth analysis of the full-width-at-half-maximum (FWHM) of the lowest angle x ray scattering peak.[1,31–33] The FWHM was computed by fitting the first diffraction peak of a-Si:H spectra.[1,29,32,33] The FWHM usually varied between 5 and 6° for all of a-Si:H samples.[1,31–33] For the t_o measurements, all a-Si:H samples were annealed up to 600 °C by ramping from room temperature to 400 °C at 10 °C/min and then from 400 °C to 600 °C at 1 °C/min. The crystallization was monitored *in situ* using an Anton Paar DHS 1100 domed hot stage. The sample was placed on the hot stage with spring clips, covered with the dome, evacuated, and purged with argon five times. Data was taken under argon atmosphere every 10 min until full crystallization was achieved (approximately after 10–12 h). Equation (1) was used to calculate crystallization content (X_c),

$$X_c = \frac{\sum_{hkl} I_{hkl}}{\sum_{hkl} I_{hkl_{MAX}}}. \quad (1)$$

TABLE I. A brief description of experimental conditions for a-Si:H films deposited at various substrate temperatures (T_{Sub}) having different R^* and hydrogen content (C_H).

T_{Sub} (°C)	d (nm)	n_{Vis}	R^*	C_H (at. %)	$\omega_{2\theta}$(°)	t_o (min)
	942	4.03	0.18		5.91	431
200 °C	1075	3.97	0.29	14 ± 1.3	5.97	384
	961	3.87	0.44		6.05	308
	1030	3.80	0.59		6.15	124
	930	4.18	0.14		5.41	308
300 °C	982	4.13	0.29	9 ± 0.8	5.64	261
	1032	4.09	0.44		5.79	214
	987	4.31	0.06		5.04	92
400 °C	975	4.29	0.10	7 ± 0.6	5.15	130
	1010	4.2	0.27		5.26	180
	1062	4.36	0.05		4.97	62
500 °C	1036	4.31	0.19	5 ± 0.4	5.06	105

Downloaded 23 Apr 2012 to 131.155.151.8. Redistribution subject to AIP license or copyright; see http://jap.aip.org/about/rights_and_permissions

$\sum I_{hkl}$ is the sum of the integrated intensities of the three orientation peaks, i.e., ⟨111⟩, ⟨220⟩, ⟨311⟩, and $\sum I_{hklMAX}$ represents the sum of the maximum intensities of all the three orientation peaks. The incubation time was chosen as the time needed to observe the c-Si XRD (111) peak rise to 1/10 of its final intensity.[1,11,34] Lift-out focused ion beam (FIB) sample preparation was performed to prepare samples for XTEM. The XTEM studies were carried out using an FEI Tecnai F30ST.

The values of thickness, refractive index, R^*, C_H, XRD FWHM, and incubation time of a-Si:H films deposited at varying substrate temperature are reported in Table I.

III. RESULTS AND DISCUSSION

A detailed analysis of the deposited films has been carried out and reported in Table I and Fig. 2. The latter shows the area of the LSM and the HSM absorption peaks as a function of R^* for different hydrogen content (C_H) values. The LSM area decreased and the HSM increased with an increase in both R^* and C_H, which is caused by a reduction of the number of divacancies and the inclusion of hydrogenated nano-sized voids. Figure 2(c) shows the corresponding XRD FWHM, $\omega_{2\theta}$, as a function of R^* for different values of C_H. Higher structural disorder in the a-Si:H films leads to a higher $\omega_{2\theta}$, because the hydrogenated nano-sized voids density increases.[1,21,35] Furthermore, $\omega_{2\theta}$ is found to increase

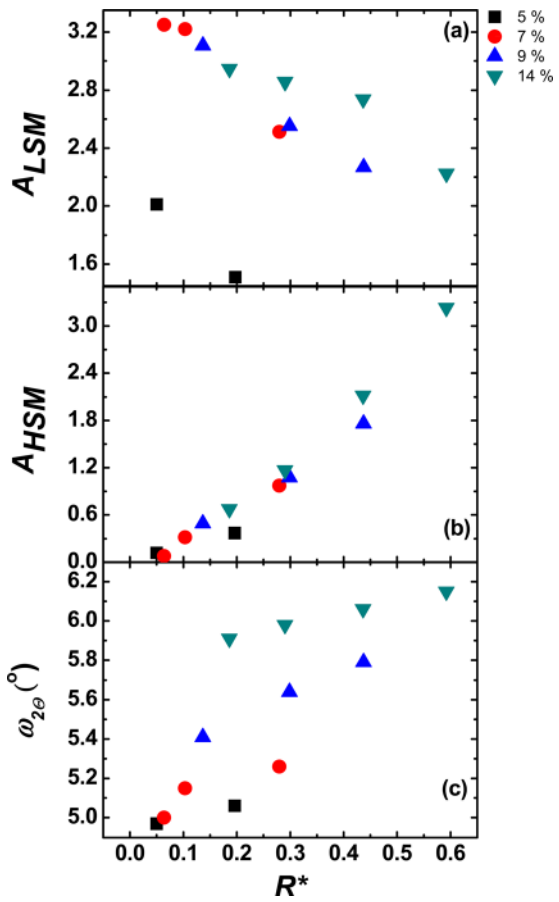

FIG. 2. (Color online) Area of the (a) LSM- and (b) HSM-related IR absorption peaks. (c) $\omega_{2\theta}$ as function of R^* for several a-Si:H films with different C_H values deposited under the experimental conditions (T_{sub}) in Table I.

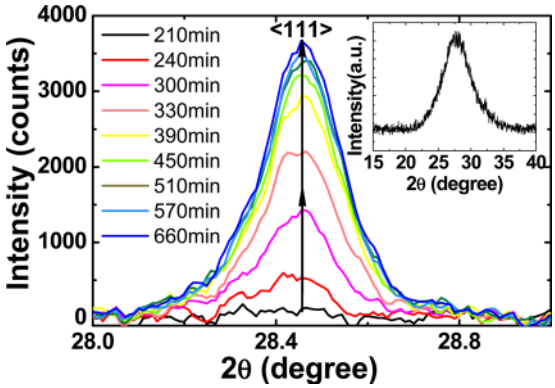

FIG. 3. (Color online) Evolution of XRD peak <111> upon crystallization for an a-Si:H film; time mentioned in the legend is the annealing time when sample reached 600 °C. XRD spectra of a-Si:H also has been shown in inset.

with an increase in C_H, due to increase in density of hydrogenated vacancies and hydrogenated nano-sized voids.

No difference in crystallization was observed in crystallization of a-Si:H films deposited on *c*-Si and Si_3N_4-coated glass substrates. However, a-Si:H films deposited on Si_3N_4-coated glass were adopted for the *in situ* crystallization kinetics study in order to get an insight into the crystallization kinetics of a-Si:H films deposited on glass. a-Si:H samples underwent a SPC treatment toward crystallization. The SPC kinetics were monitored by means of *in situ* XRD. Figure 3 shows the evolution of the XRD peaks during annealing. For comparison, a XRD peak for an a-Si:H sample has been shown in the inset of Fig. 3. All samples were fully crystallized after *in situ* annealing as inferred by Raman spectroscopy, as shown in Fig. 4 along with spectra for an a-Si:H film. Furthermore, Fig. 5(a) shows an example of the evolution of the X_C as a function of the annealing time for one value of MRO and C_H. Figure 5(b) shows the relation between t_o and $\omega_{2\theta}$ (since MRO controls t_o); under conditions of high MRO ($\omega_{2\theta} < 5.5$), the t_o inversely correlate with the MRO, i.e., the larger the MRO, the smaller the t_o. However, for progressively larger values of $\omega_{2\theta}$, the t_o appeared to decrease, suggesting that the crystallization kinetics in films characterized by large $\omega_{2\theta}$ and higher R^* ($\geq$ 0.3) values are not solely controlled by the MRO. Therefore,

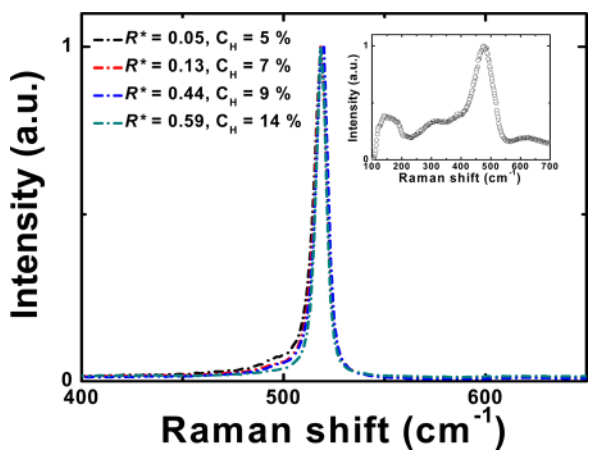

FIG. 4. (Color online) Raman spectra of fully crystallized poly-Si films; inset shows a typical Raman spectra of a-Si:H.

Downloaded 23 Apr 2012 to 131.155.151.8. Redistribution subject to AIP license or copyright; see http://jap.aip.org/about/rights_and_permissions

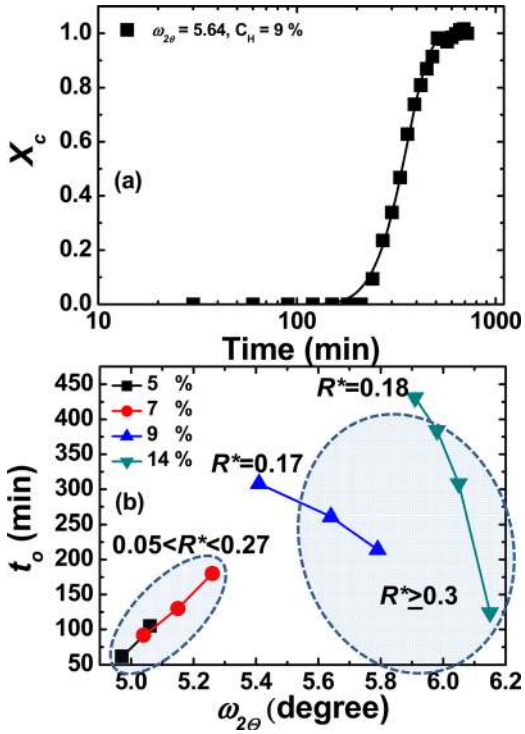

FIG. 5. (Color online) (a) Crystalline content (X_c) as function of the annealing time (600 °C). The solid line is a fit to the data using the approach described by Iverson and Reif (Ref. 6). (b) Incubation time (t_o) as a function of the FWHM ($\omega_{2\theta}$) for different a-Si:H films along with R* values deposited under the experimental conditions (T_{sub}) reported in Table I; solid lines are guide to the eye.

because of the unexpected trend, selected a-Si:H layers were characterized during two steps of annealing, i.e., at 450 °C and 550 °C for 10 min. Figures 6(a) and 6(b) shows the changes in the LSM and HSM modes upon annealing, as measured by means of Raman spectroscopy, for two films with a C_H of 14% and different R^* values, 0.18 and 0.6, respectively. Upon annealing, the HSM intensity was found to decrease drastically when compared to the LSM intensity. This observation is supported by the fact that hydrogen associated with nano-sized voids starts to diffuse out at

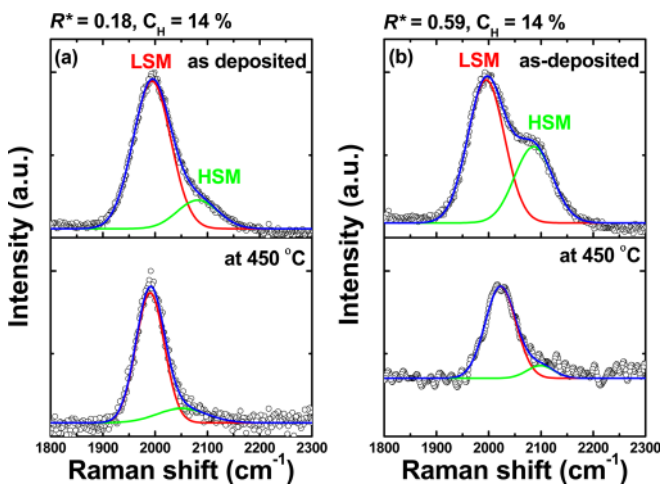

FIG. 6. (Color online) Raman spectra of the as-deposited and annealed (a) low R^* and (b) high R^* a-Si:H films, both with a hydrogen content of 14%.

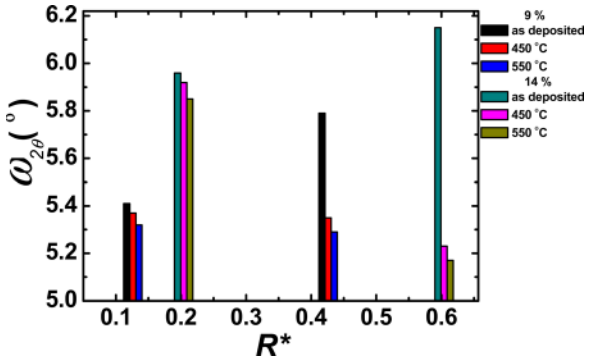

FIG. 7. (Color online) The FWHM ($\omega_{2\theta}$) upon annealing as function of R^* for a-Si:H films characterized by a C_H of 9 and 14 at. %.

150–400 °C, whereas hydrogen present in divacancies escapes around 550–600 °C.[36] It can be, therefore, concluded that the films with a larger concentration of nano-voids, i.e., higher values of R^*, undergo larger structural changes upon annealing.[36–40]

To further investigate the impact of the hydrogen out-diffusion in high R^* films, *ex situ* XRD measurements were also carried out on the samples after annealing at 450 °C and 550 °C. Figure 7 shows the change in $\omega_{2\theta}$ during annealing as a function of R^* for different C_H values. The MRO is found to increase upon annealing for the films characterized by a higher R^*. This suggests that, in highly disordered films, nanosized voids collapse upon hydrogen out-diffusion, leading to a more compact structure, characterized by a larger MRO. This leads eventually to shorter t_o, as previously observed in Fig. 5(b).

Furthermore, in order to investigate the effect of t_o on the grain size of poly-Si, cross-sectional transmission electron microscopy (XTEM) measurements were carried out on low and high R^* samples, as shown in Fig. 8. Large grains are evident for high R^* films, as compared to low R^* films. A quantitative data analysis in terms of the average and maximum grain size as a function of R^* for different C_H values is shown in Fig. 9. Despite the shorter t_o, a-Si:H films characterized by high values of R^* (0.44 and 0.60) lead to the development of larger grains than the films characterized by a lower R^* and longer t_o. This additional experimental evidence confirms the results presented in Ref. 22, i.e., R^*

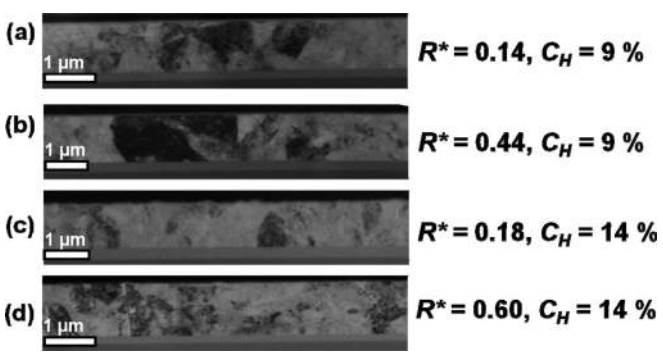

FIG. 8. XTEM images of poly-Si films crystallized from a-Si:H films having low and high R* values: (a) $R^* = 0.14$, $C_H = 9\%$; (b) $R^* = 0.44$, $C_H = 9\%$; (c) $R^* = 0.18$, $C_H = 14\%$; (d) $R^* = 0.60$, $C_H = 14\%$.

Downloaded 23 Apr 2012 to 131.155.151.8. Redistribution subject to AIP license or copyright; see http://jap.aip.org/about/rights_and_permissions

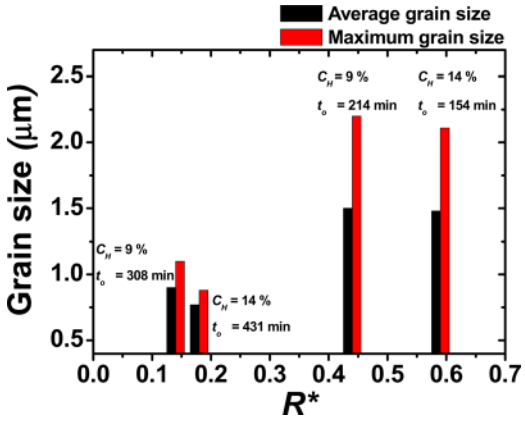

FIG. 9. (Color online) The variation of the maximum and average grain size as function of R^* for a-Si:H films characterized by a C_H of 9 and 14 at. %.

controls the final grain size in poly-Si. While the role of MRO in controlling the incubation time is acknowledged, it is also concluded that the evaluation of the MRO of the pristine a-Si:H is not sufficient to predict the incubation time, since highly disordered layers (i.e., $R^* \geq 0.3$) undergo a massive hydrogen out-diffusion process from the nanosized voids, accompanied by a restructuring of the network and an increase in the MRO during the annealing procedure.

IV. CONCLUSIONS

An extensive material analysis has been carried out by means of SE, FTIR, XTEM, Raman, and XRD on a-Si:H films prior and upon SPC crystallization toward the development of poly-Si layers. This study has allowed us to investigate the effect of the a-Si:H structure, i.e., MRO and the microstructure parameter R^*, on the crystallization process in terms of t_o and final grain size. The set of experimental data here presented has confirmed the role of R^* in controlling the final grain size. Furthermore, the choice of an extended range of the microstructure parameter R^* (0.05-0.6) has allowed us to highlight the role of the MRO and nanosized voids in controlling the t_o. For films characterized by low R^* $(0.05 < R^* < 0.3)$, the crystallization results show that t_o increases with a decrease in MRO, in agreement with literature.[1] However, for progressively disordered layers ($R^* \geq 0.3$), the t_o is found to decrease along with a further decrease in the MRO of the pristine a-Si:H. This unexpected result has been attributed to the hydrogen out-diffusion from the nanosized voids upon annealing, as pointed out by Raman analysis. The hydrogen out-diffusion induces a collapse in the silicon network, which leads to an improved MRO in the annealed a-Si:H layer and, therefore, a shorter t_o. In this respect, the novelty of these results is providing evidence that the t_o is not solely controlled by the MRO parameter of the pristine a-Si:H. Instead, nanosized voids are actively involved in controlling the nucleation step, since they induce a restructuring of the a-Si:H layer upon annealing. These results are partially in contrast with the work by Mahan *et al.*,[1] where it is generally concluded that the microstructure of the a-Si:H layer (i.e., presence of nano-sized voids) does not influence the crystallization process.

ACKNOWLEDGMENTS

This work was carried out with a subsidy of the Dutch Ministry of Economic Affairs under the EOS-LT program (project number EOSLT06029). The authors acknowledge M. J. F. van de Sande, J. J. L. M. Meulendijks, W. Keuning, and J. J. A. Zeebregts for their technical support. This research has been made possible within the project NOVASIL founded by Agentschap.nl (former SenterNovem).

[1]A. H. Mahan, T. N. Su, D. L. Williamson, L. M. Gedvilas, S. P. Ahrenkiel, P. A. Parilla, Y. Q. Xu, and D. A. Ginley, Adv. Funct. Mater. **19**, 2338 (2009).
[2]R. B. Bergmann, G. Oswald, M. Albrecht, and V. Gross, Sol. Energy Mater. Sol. Cells **46**, 147 (1997).
[3]M. A. Green, Appl. Phys. A **96**, 153 (2009).
[4]A. Illiberi, K. Sharma, M. Creatore, and M. C. M. van de Sanden, Mater. Lett. **63**, 1817 (2009).
[5]M. A. Green, P. A. Basore, N. Chang, D. Clugston, R. Egan, R. Evans, D. Hogg, S. Jarnason, M. Keevers, P. Lasswell, J. O'Sullivan, U. Schubert, A. Turner, S. R. Wenham, and T. Young, Sol. Energy **77**, 857 (2004).
[6]R. B. Iverson and R. Reif, J. Appl. Phys. **62**, 1675 (1987).
[7]M. K. Hatalis and D. W. Greve, J. Appl. Phys. **63**, 2260 (1988).
[8]H. Y. Kim, K. Y. Lee, and J. Y. Lee, Thin Solid Films **302**, 17 (1997).
[9]H. Y. Kim, J. B. Choi, and J. Y. Lee, J. Vac. Sci. Technol. A **17**, 3240 (1999).
[10]J. N. Lee, B. J. Lee, D. G. Moon, and B. T. Ahn, Jpn. J. Appl. Phys. **36**, 6862 (1997).
[11]A. H. Mahan, B. Roy, R. C. Reedy, D. W. Readey, and D. S. Ginley, J. Appl. Phys. **99**, (2006).
[12]A. H. Mahan, S. P. Ahrenkiel, R. E. I. Schropp, H. Li, and D. S. Ginley, Thin Solid Films **516**, 529 (2008).
[13]K. Nakazawa and K. Tanaka, J. Appl. Phys. **68**, 1029 (1990).
[14]D. Y. Song, D. Inns, A. Straub, M. L. Terry, P. Campbell, and A. G. Aberle, Thin Solid Films **513**, 356 (2006).
[15]A. H. M. Smets, W. M. M. Kessels, and M. C. M. van de Sanden, Appl. Phys. Lett. **82**, 1547 (2003).
[16]S. Chakraborty and D. A. Drabold, Phys. Rev. B **79**, 115214 (2009).
[17]P. Biswas and R. Timilsina, J. Phys.: Condens. Matter **23**, 065801 (2011).
[18]R. Timilsina and P. Biswas, Phys. Status Solidi A **207**, 609 (2010).
[19]S. R. Elliott, J. Phys.: Condens. Matter **4**, 7661 (1992).
[20]T. C. Hufnagel, Nature Mater. **3**, 666 (2004).
[21]A. Uhlherr and S. R. Elliott, Philos. Mag. B **71**, 611 (1995).
[22]K. Sharma, A. Branca, A. Illiberi, F. D. Tichelaar, M. Creatore, and M. C. M. van de Sanden, Adv. Energy Mater. **1**, 401 (2011).
[23]W. M. M. Kessels, R. J. Severens, A. H. M. Smets, B. A. Korevaar, G. J. Adriaenssens, D. C. Schram, and M. C. M. van de Sanden, J. Appl. Phys. **89**, 2404 (2001).
[24]M. C. M. van de Sanden, R. J. Severens, J. Bastiaanssen, and D. C. Schram, Surf. Coat. Technol. **97**, 719 (1997).
[25]G. D. Cody, T. Tiedje, B. Abeles, T. D. Moustakas, B. Brooks, and Y. Goldstein, J. Phys. (Paris) **42**, 301 (1981).
[26]A. H. M. Smets, W. M. M. Kessels, and M. C. M. van de Sanden, J. Appl. Phys. **102**, 073523 (2007).
[27]S. Guha, J. Yang, D. L. Williamson, Y. Lubianiker, J. D. Cohen, and A. H. Mahan, Appl. Phys. Lett. **74**, 1860 (1999).
[28]A. H. Mahan, J. Yang, S. Guha, and D. L. Williamson, Phys. Rev. B **61**, 1677 (2000).
[29]A. H. Mahan, R. Biswas, L. M. Gedvilas, D. L. Williamson, and B. C. Pan, J. Appl. Phys. **96**, 3818 (2004).
[30]P. M. Voyles and J. R. Abelson, Sol. Energy Mater. Sol. Cells **78**, 85 (2003).
[31]M. Netrvalova, V. Vavrunkova, J. Mullerova, and P. Sutta, J. Electr. Eng.: Elektrotechnicky Cas. **60**, 279 (2009).
[32]V. Vavrunkova, G. van Elzakker, M. Zeman, and P. Sutta, Phys. Status Solidi A **207**, 548 (2010).
[33]M. Zeman, G. van Elzakker, F. D. Tichelaar, and P. Sutta, Philos. Mag. **89**, 2435 (2009).
[34]B. Roy, A. H. Mahan, Q. Wang, R. Reed, D. W. Readey, and D. S. Ginley, Thin Solid Films **516**, 6517 (2008).

Downloaded 23 Apr 2012 to 131.155.151.8. Redistribution subject to AIP license or copyright; see http://jap.aip.org/about/rights_and_permissions

[35]S. R. Elliott, in *Encyclopedia of Materials: Science and Technology*, edited by K. H. Jnrgen Buschow, W. C. Robert, C. F. Merton, P. B. Ilschner, J. K. Edward, M. Subhash, and U. P. Veyssière (Elsevier, Oxford, 2001), p. 186.
[36]W. C. Hsiao, C. P. Liu, and Y. L. Wang, J. Electrochem. Soc. **154**, G122 (2007).
[37]W. Beyer and H. Wagner, J. Phys. (Paris) **42**, 783 (1981).
[38]W. Beyer, H. Wagner, J. Chevallier, and K. Reichelt, Thin Solid Films **90**, 145 (1982).
[39]N. Sridhar, D. D. L. Chung, W. A. Anderson, and J. Coleman, J. Electron. Mater. **24**, 1451 (1995).
[40]N. Budini, P. A. Rinaldi, J. A. Schmidt, R. D. Arce, and R. H. Buitrago, Thin Solid Films **518**, 5349 (2010).

Downloaded 23 Apr 2012 to 131.155.151.8. Redistribution subject to AIP license or copyright; see http://jap.aip.org/about/rights_and_permissions